ISSN 2278-2540 | DOI: 10.51583/IJLTEMAS | Volume XV, Issue IV, April 2026

Cat Swarm Optimization-Based Optimal Placement of FACTS (UPFC) For Voltage Stability Improvement in Power System

Usman Babagana*, Isarar Ahmad

Department of Electrical Engineering, FE & IT, Integral University, 226026 Lucknow, India

***Corresponding Author**

DOI: https://doi.org/10.51583/IJLTEMAS.2026.150400020

Received: 06 April 2026; 11 April 2026; Published: 02 May 2026

ABSTRACT

The present paper suggests a Cat Swarm Optimization (CSO)-based model of optimal placement and parameter adjustment of a Unified Power Flow Controller (UPFC) to improve voltage stability in power systems under normal operating conditions as well as N-1 contingency operating conditions. The most flexible combined series-shunt FACTS controller, the UPFC, controls the magnitude of voltage, the line impedance and the phase angle simultaneously by coordinated series voltage injection and shunt reactive power compensation. The L-index of the partitioned bus admittance matrix is used to measure the voltage stability, and the worst-case contingency value L worst is used as the optimization fitness function. The CSO algorithm, which works based on dual seeking and tracing the behavioral modes, reduces L worst to UPFC placement and parameter constraints without the need to have the gradient information. The model has been confirmed in the IEEE 14-bus and in the IEEE 30-bus benchmark systems that are simulated in MATLAB/MATPOWER. Findings indicate that UPFC integration reduced the L-index by 0.26% in the IEEE 14-bus and 0.54% in the IEEE 30-bus system at normal and then CSO-optimized UPFC location leads to 4.28% reduction in the worst-case L-index at N-1 contingency on the IEEE 14-bus system and 24.85% on the IEEE 30-bus system. Optimization increased voltage profiles on all buses to the nominal 1.0 p.u. These results support the claim that the proposed CSO-UPFC framework is a computationally efficient and practically viable approach towards enhancing voltage security of the power system both when it is operating in normal conditions and when it is subjected to disturbances.

Keywords: IEEE 14 & 30 Bus systems, Voltage stability index, FACTS (UPFC) devices, Cat Swarm Optimization (CSO), N-1 contingency analysis, MATPOWER.

INTRODUCTION

The high demand of power, regional grid interconnection and integration of large-scale renewable energy are driving modern power systems to operate just below their thermal and stability margins [1]. In these stressed conditions, contingencies such as transmission line faults, generator failures and unforeseen switching events can cause severe degradation of the voltage profiles, lead to reactive power shortages and cause cascading voltage collapses [2][3]. Voltage stability, which is formally defined by the IEEE/CIGRE Joint Task Force as the ability of the system to sustain acceptable bus voltages after a given disturbance has occurred has become a major research imperative in the contemporary power engineering [4].

Originally proposed by Hingorani [5], Flexible AC Transmission System (FACTS) devices provide dynamic reactive compensation of power and controllability of the power flow. The Unified Power Flow Controller (UPFC) is the most versatile series-shunt controller with shunting capability that can simultaneously regulate the magnitude of voltage, line impedance, and phase angle [6]. FACTS devices enhance voltage profiles, enhance system loadability, and minimise transmission losses during normal and contingency conditions [7][8]. Their performance is however very sensitive to the location of the network and thus optimal siting is a complex nonlinear optimization problem [5][6][9].

ISSN 2278-2540 | DOI: 10.51583/IJLTEMAS | Volume XV, Issue IV, April 2026

To solve this, the current work suggests a Cat Swarm Optimization (CSO)-based method of solving the optimal site and parameter configuration of UPFC devices. The swarm intelligence metaheuristic, CSO, was first introduced by Chu et al. in 2006 [10], which has two behavioral modes, namely, seeking (local exploitation) and tracing (global exploration), which allows robust convergence in nonlinear power system problems without the use of gradient information [11][12]. It is straightforward, converges quickly, and can search across the globe and is therefore suited to FACTS placement problems [13].

STEADY-State load flow analysis is done on the proposed methodology on the standard IEEE 14-bus and IEEE 30-bus benchmark test systems in MATPOWER [14]. Performance evaluation includes reduction of voltage deviation, reduction of real power loss, and improvement of voltage stability index under normal operating conditions of base-case and N-1 contingency

METHODOLOGY

The proposed methodology combines eight systematic steps which are power system modeling, load flow analysis, voltage stability analysis, FACTS/UPFC modeling, N-1 contingency analysis, optimization problem formulation, CSO implementation and MATLAB/MATPOWER execution as shown in Figure 3.1. The framework is run on two standard IEEE benchmark networks, and run fully in MATLAB via MATPOWER.

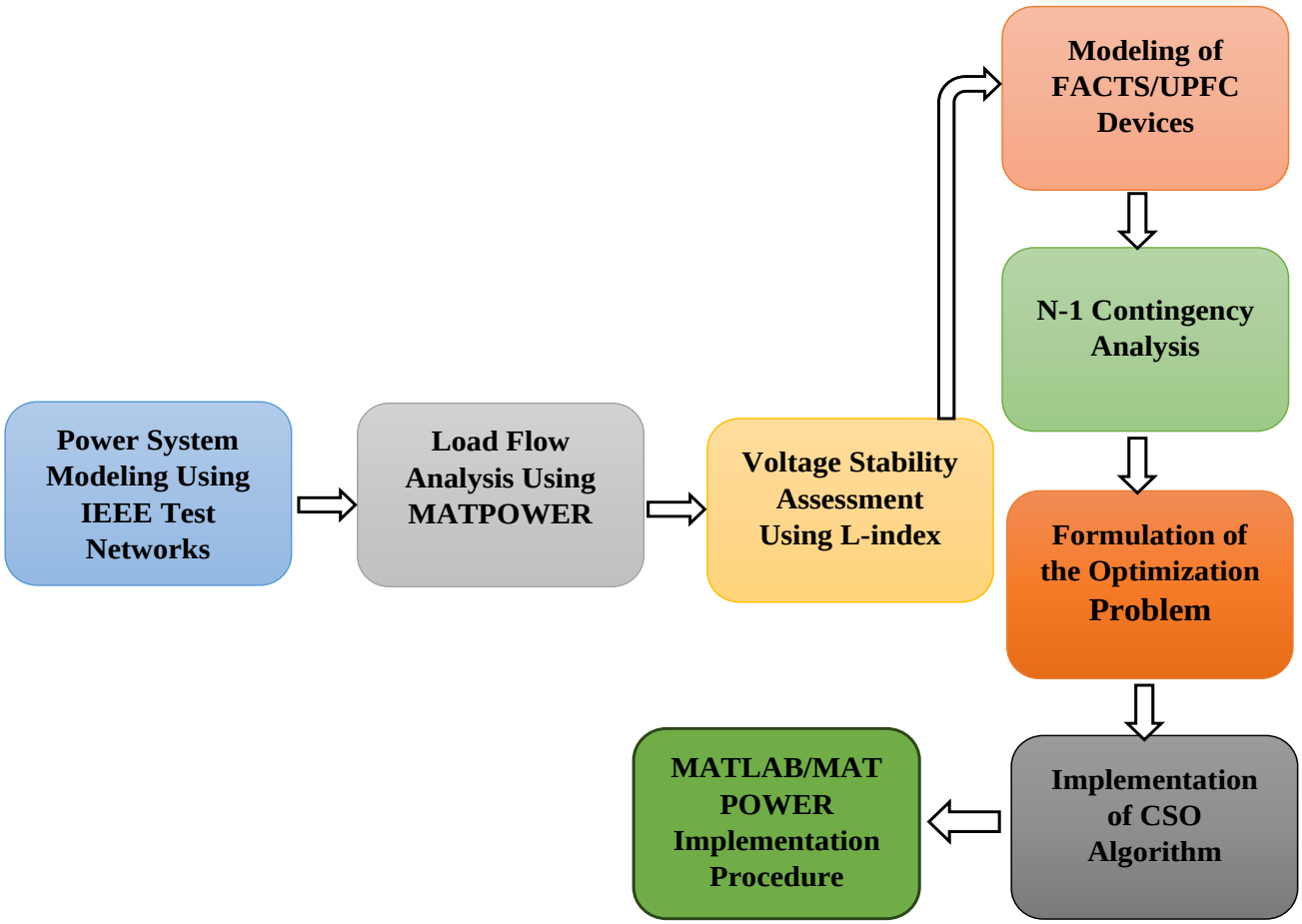

Figure 3.1: Methodology Block Diagram

Power System Modeling

Two benchmark networks are used to validate. IEEE 14-bus system includes 14 buses, 5 generators, 11 loads and 20 transmission lines, as shown in Figure 1 (IEEE 14-bus model). Figure 2 represents a more detailed network with 30 buses, 6 generators, 24 loads and 41 transmission lines, and is known as the IEEE 30-bus system [15].

ISSN 2278-2540 | DOI: 10.51583/IJLTEMAS | Volume XV, Issue IV, April 2026

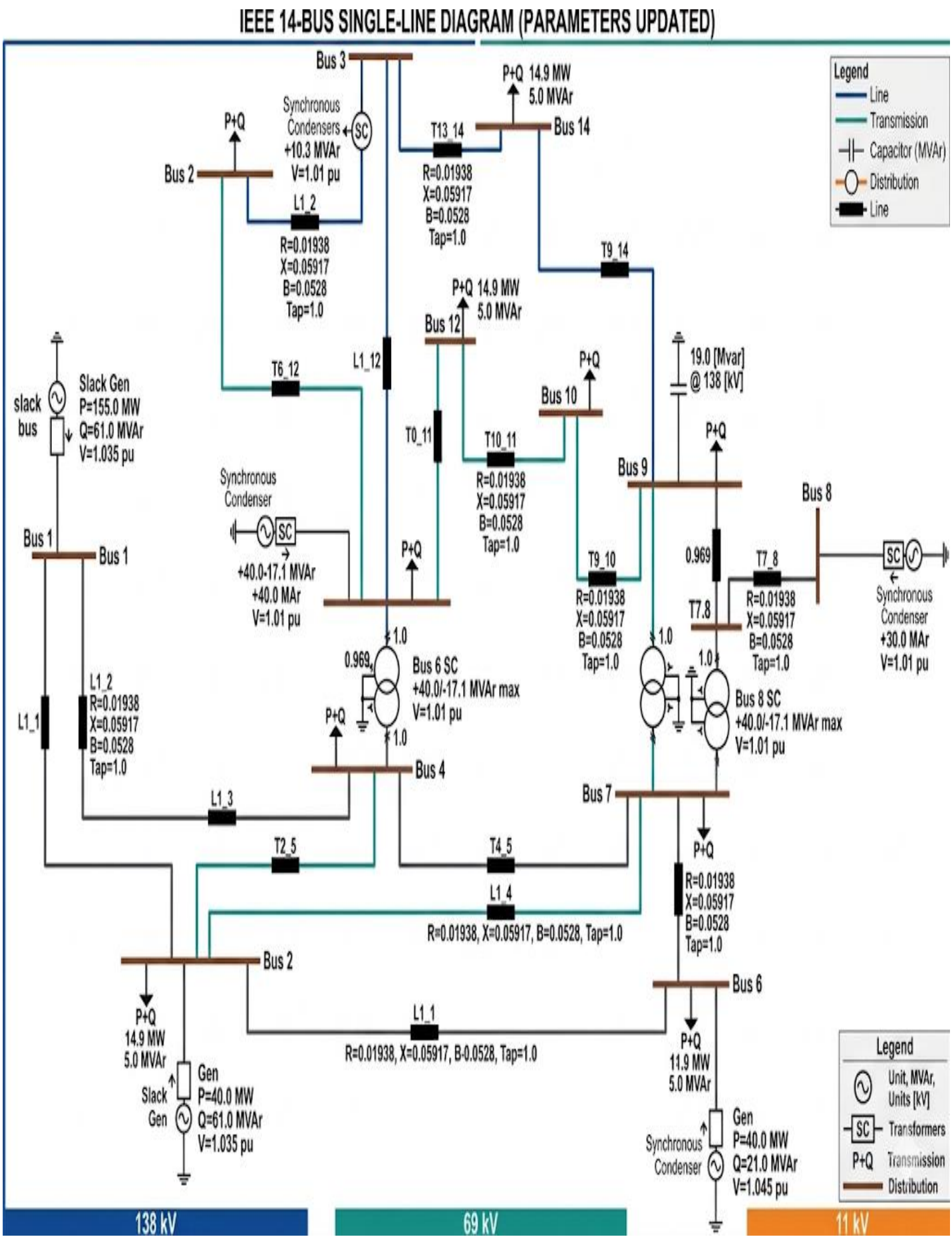

Figure 1. A Model of the IEEE 14-bus system

ISSN 2278-2540 | DOI: 10.51583/IJLTEMAS | Volume XV, Issue IV, April 2026

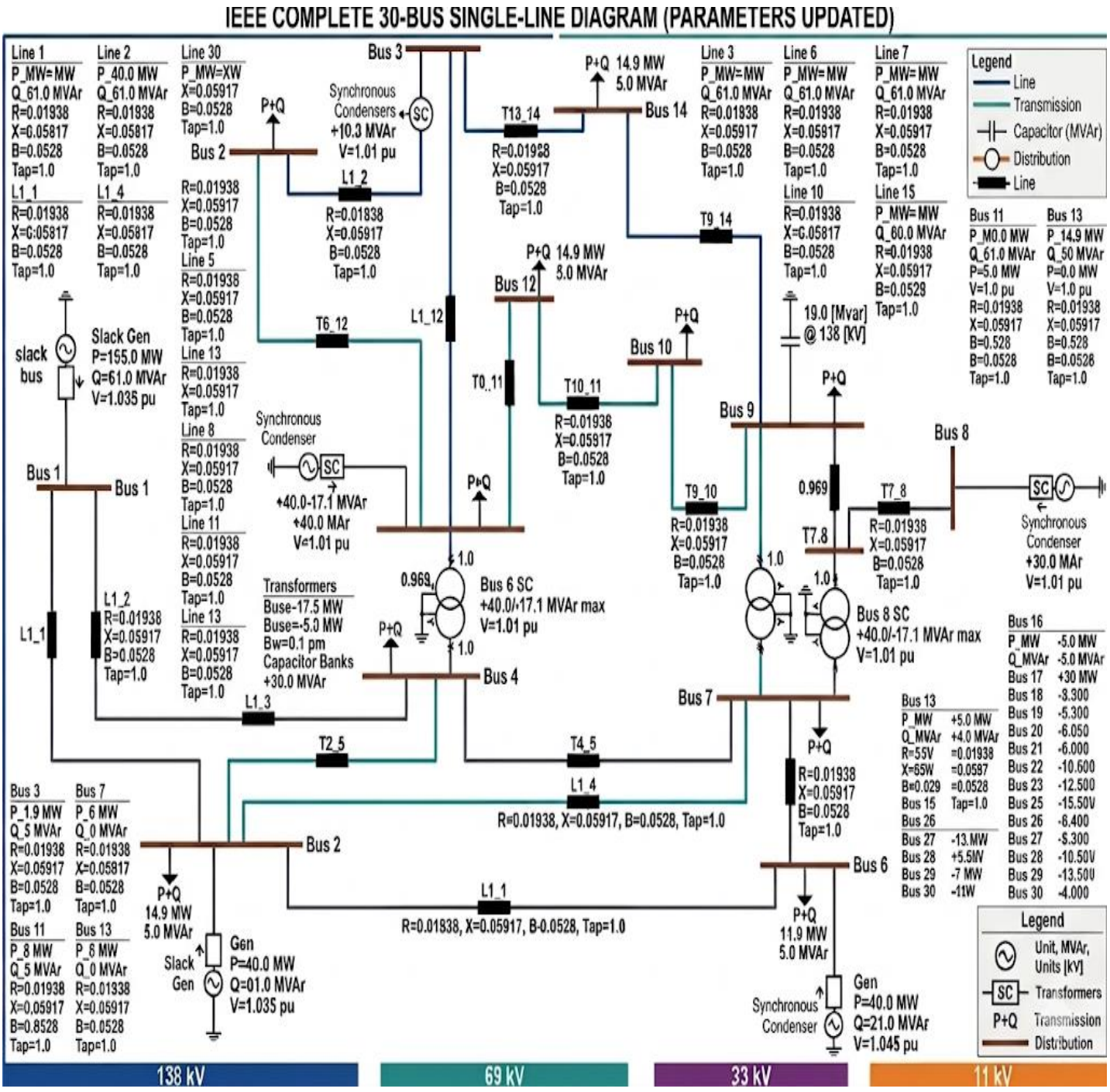

Figure 2: A depicted part of the IEEE 30-bus system.

Power Flow Analysis

Load flow analysis determines bus voltage magnitudes, angles, and line power flows. The active and reactive power balance at each bus is governed by the Newton-Raphson nonlinear equations implemented in MATPOWER, expressed as **Equations (1) and (2):**

$$P_i = V_i \sum_{j=1}^{N} V_j \left(G_{ij} \cos \theta_{ij} + B_{ij} \sin \theta_{ij} \right) \quad (1)$$

$$Q_i = V_i \sum_{j=1}^{N} V_j \left(G_{ij} \cos \theta_{ij} - B_{ij} \sin \theta_{ij} \right) \quad (2)$$

ISSN 2278-2540 | DOI: 10.51583/IJLTEMAS | Volume XV, Issue IV, April 2026

Where:

P_i = real power injection at bus i
Q_i = reactive power injection at bus i
V_i = voltage magnitude at bus i
V_j = voltage at generator bus j
G_{ij} = conductance between buses i and j
B_{ij} = susceptance between buses i and j

Voltage Stability Assessment

Voltage stability is analyzed through the P-V curve relationship modeled by **Equation (3)** [3]:

$$P = \frac{V_s V_r}{X} \sin \delta \tag{3}$$

In Equation (4), the voltage stability margin (VSM) is defined. The voltage instability is represented by the singularity of Jacobian matrix, which is represented as a load flow Jacobian as expressed in Equation (5) [16].

$$VSM = P_{max} - P_{operating} \tag{4}$$

Where:

P_{max}= the maximum can be transferred before collapse.

$$\det(J) = 0 \tag{5}$$

Where:

$$J = \begin{bmatrix} \frac{\partial P}{\partial \delta} & \frac{\partial P}{\partial V} \\ \frac{\partial Q}{\partial \delta} & \frac{\partial Q}{\partial V} \end{bmatrix}$$

The L-index is obtained by partitioning the bus admittance matrix in Equation (6) and the transfer matrix F in Equation (7) and is the main scalar measure of stability [16]. L-index is determined at every load bus i by calculating Equation (8):

$$\begin{bmatrix} I_G \\ I_L \end{bmatrix} = \begin{bmatrix} Y_{GG} & Y_{GL} \\ Y_{LL} & Y_{LL} \end{bmatrix} \begin{bmatrix} V_G \\ V_L \end{bmatrix} \tag{6}$$

From this, the matrix F is obtained as:

$$F = -Y_{LL}^{-1} Y_{LG} \tag{7}$$

$$L_i = \left| 1 - \sum_{j \in G} F_{ij} \frac{V_j}{V_i} \right| \tag{8}$$

Where:

L_i = voltage stability index at load bus i

F_{ij} = elements derived from the network admittance matrix

V_j = voltage at generator bus j

V_i = voltage at load bus i

ISSN 2278-2540 | DOI: 10.51583/IJLTEMAS | Volume XV, Issue IV, April 2026

The system-wide stability indicator is the largest of all load buses, which is given in Equation (9). The interpretation of L-index values is as follows, 0 represents a stable system, 0.2-0.5 represents a moderate stress, and 0.5-1.0 represents the approach to a voltage collapse [16].

$$L_{max} = max(L_i) \tag{9}$$

FACTS/UPFC Modeling

FACTS devices are actively controlled devices which control the flow of power by Equation (3), $P = \frac{V_i V_j}{X} \sin \delta$ by regulating voltage V, reactance X [8]. by regulating voltage V, reactance X, or phase angle δ [6][7][8]. Voltage impact Shunt controllers inject reactive power according to Equations (10) and (11), changing the bus reactive power balance according to Equation (12), and voltage impact is described according to Equation (13) [16]. The series controllers adjust the effective line reactance according to Equation (14) to adjust the power transfer and reactive flow according to Equations (15) and (16) [98. Combined series-shunt controllers, such as the UPFC, use the general model of power injection of equation (17) and (12), where power flow is adjusted in equation (18) [6][8]. Phase angle regulators are based on the model of Equation (19) [7].

$$Q_{sh} = V^2 B_{sh} \tag{10}$$

$$Q_{sh} = V I_{sh} \tag{11}$$

Where:

V = bus voltage
Q_{sh} = shunt reactive power injected
B_{sh} = controllable susceptance
I_{sh} = injected current

$$Q_i^{new} = Q_i + Q_{sh} \tag{12}$$

$$\Delta V \propto \frac{Q_{sh}}{V} \tag{13}$$

$$X_{eff} = X + X_{se} \tag{14}$$

$$P_{ij} = \frac{V_i V_j}{X_{eff}} \sin(\delta_i - \delta_j) \tag{15}$$

$$Q_{ij} = \frac{V_i^2}{X_{eff}} - \frac{V_i V_j}{X_{eff}} \cos(\delta_i - \delta_j) \tag{16}$$

Where:

δ_i, δ_j = voltage angles

$$P_i^{new} = P_i + P_{inj} \tag{17}$$

$$P_{ij} = \frac{V_i V_j}{X_{eff}} \sin(\delta_i - \delta_j + \emptyset) \tag{18}$$

Where:

$X_{eff} = X + X_{se}$

$\emptyset$ = injected phase angle

ISSN 2278-2540 | DOI: 10.51583/IJLTEMAS | Volume XV, Issue IV, April 2026

$$P_{ij} = \frac{V_i V_j}{X} \sin(\delta_i - \delta_j + \theta) \quad (19)$$

Where:

θ = injected phase shift

Figure 3 is the structural topology of the UPFC, which is composed of two Voltage Source Converters (VSCs) connected by a common DC link of a series-connected SSSC and a shunt-connected STATCOM [7]. The equations above (20) and (21) define base-case power flow on a line between bus i and bus j. When UPFC is installed, the series voltage injection in Equation (22) changes the effective sending-end voltage according to Equation (23), resulting in the UPFC controlled power flow in Equation (24) and its expanded form in Equation (25), which simultaneously governs the magnitude of voltages, line impedance, and phase angle. The shunt converter offers reactive power support in accordance with Equation (11) and adjusts the bus reactive balance according to Equation (12).

$$P_{ij} = \frac{V_i V_j}{X_{ij}} \sin(\delta_i - \delta_j) \quad (20)$$

$$Q_{ij} = \frac{V_i^2}{X_{ij}} - \frac{V_i V_j}{X_{ij}} \cos(\delta_i - \delta_j) \quad (21)$$

$$V_{se} = |V_{se}| \angle \delta \quad (22)$$

$$V_i' = V_i + V_{se} \quad (23)$$

$$P_{ij}^{UPFC} = \frac{V_i' V_j}{X_{ij}} \sin(\delta_i' - \delta_j) \quad (24)$$

$$P_{ij}^{UPFC} = \frac{(V_i + V_{se}) V_j}{X_{ij}} \sin(\delta_i - \delta_j + \theta) \quad (25)$$

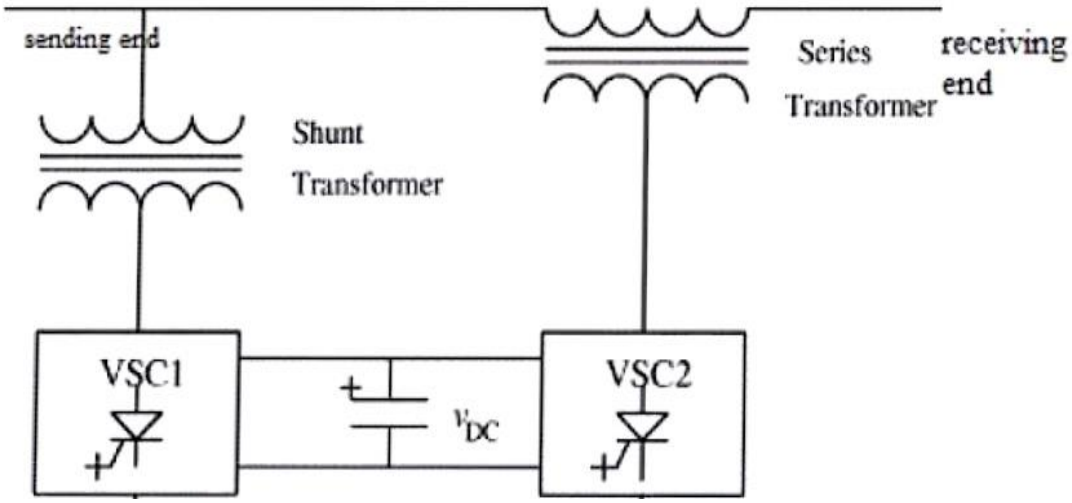

Figure 3. A Structure of UPFC

N-1 Contingency Analysis

N-1 security criterion takes into consideration that the network should be able to sustain the failure of any of the transmission lines [3]. Base-case power flow is repeated each time a line outage occurs and the line is removed, post contingency power flow is executed, and the L-index calculated. Equation (26) represents the worst-case stability index in all contingencies

ISSN 2278-2540 | DOI: 10.51583/IJLTEMAS | Volume XV, Issue IV, April 2026

$$L_{worst} = max(L_{contingency}) \quad (26)$$

This L_{worst} value constitutes the fitness function for optimization.

Optimization Problem Formulation

The optimization problem is the minimization of L worst, subject to four operational constraints; UPFC line location, Equation (27), series reactance injection, Equation (28), reactive power injection, Equation (29), and bus location, Equation (30).

$$1 \leq Line_{UPFC} \leq N_{lines} \quad (27)$$

$$X_{min} \leq X_{inj} \leq X_{max} \quad (28)$$

$$Q_{min} \leq Q_{inj} \leq Q_{max} \quad (29)$$

$$1 \leq Bus_{UPFC} \leq N_{bus} \quad (30)$$

Cat Swarm Optimization Implementation

CSO [10][12] encodes each candidate solution as a four-variable vector per **Equation (31):**

$$X = [Line, X_{inj}, Q_{inj}, Bus] \quad (31)$$

Where:

Line = Transmission line where UPFC is installed

X_{inj} = Series reactance injection

Q_{inj} = Reactive power injection

Bus = Bus location of shunt compensation

Thus, the position of each cat corresponds to a specific UPFC configuration applied to the network.

Equation (32) is used to initialize the population randomly within the bounds of variables. Fitness is determined as Fitness = L worst per Equation (33). The mode of seeking (70%), mode of tracing (30%) is assigned to cats through a Mixture Ratio MR = 0.3, as shown in Equations (34) and (35). In seeking mode, positions of candidate are disturbed according to Equation (36) with SRD = 0.2. Position is modified in tracing mode to the global best as in Equation (37). Equations (38) and (39) are used to apply boundary enforcement, and Equation (40) is used to update the global best. Table 1 presents the CSO parameter settings, which have been chosen according to the literature recommendations and exploratory trials [10].

Table 1 CSO Parameters

Parameter	Value
Population size	20
Maximum iterations	50
Mixture ratio (MR)	0.3
Seeking range dimension (SRD)	0.2
Counts of dimension change (CDC)	0.8
Seeking memory pool (SMP)	5

ISSN 2278-2540 | DOI: 10.51583/IJLTEMAS | Volume XV, Issue IV, April 2026

$$X_i = X_{min} + rand() \times (X_{max} - X_{min}) \quad (32)$$

Where:

X_i = Position of cat i

X_{min} and X_{max} = Lower and upper bounds of variables.

$$Fitness = L_{worst} \quad (33)$$

Where:

L_{worst} = the maximum L-index obtained under contingency scenarios.

The assignment is controlled using the Mixture Ratio (MR) parameter.

$$M.R = \frac{Number\ of\ tracing\ cats}{Total\ cats} \quad (34)$$

$$M.R = 0.3 \quad (35)$$

$$X_{candidate} = X_{current} + SRD \times rand() \quad (36)$$

Where:

SRD = Seeking Range of Selected Dimension
Rand () = random number between −1 and 1

$$X_i^{new} = X_i + r(X_{best} - X_i) \quad (37)$$

Where:

X_i = current cat position

X_{best} = global based solution

r = random number between 0 and 1

$$X = \max(X, X_{min}) \quad (38)$$

$$X = \min(X, X_{max}) \quad (39)$$

$$X_{best} = argmin(Fitness) \quad (40)$$

RESULTS AND DISCUSSION

The outcomes of the simulation assess the CSO-optimal framework of the UPFC placement on the IEEE 14 benchmark and IEEE 30 benchmark system. The performance is measured under three conditions, which include base case, normal operation with UPFC, and N-1 contingency with CSO-optimized location of UPFC.

Base Case Voltage Stability Assessment

Before optimization, the base case load flow analysis was used to determine reference values of L-index of the two-test system. Base case L-index of the IEEE 14-bus system was 0.0768, and the IEEE 30-bus system was 0.0553, which means that both systems will work within stable margins when loaded normally. This reflects the relatively greater base case voltage stability margin of the IEEE 30-bus system in the lower value, but the systems are both vulnerable to degradation under contingency conditions.

ISSN 2278-2540 | DOI: 10.51583/IJLTEMAS | Volume XV, Issue IV, April 2026

UPFC Performance Under Normal Operating Conditions

Under normal operating conditions, which followed the installation of the UPFC, marginal yet significant decreases of the maximum L-index were found in the two systems as indicated in Table .2. The IEEE 14-bus system improved from 0.0768 to 0.0766, while the IEEE 30-bus system improved from 0.0553 to 0.0550.

These are equivalent to 0.26% and 0.54% improvements in voltage stability respectively as quantified in Table 3. The stronger enhancement in IEEE 30-bus system is explained by the higher voltages variability of larger networks whose conditions are under load. Though the gains are numerically small they are operationally important, especially when the loadings are greater or when the stress due to contingencies occur [6].

Table 2. UPFC Performance Under Normal Operating Conditions

Test System (Normal)	Base Case L-index	With UPFC
IEEE 14 Bus	0.0768	0.0766
IEEE 30 Bus	0.0553	0.0550

Table 3. Voltage Stability Improvement Analysis (Normal)

Test System	Base Case	Normal with UPFC	Improvement
IEEE 14 Bus	0.0768	0.0766	0.26%
IEEE 30 Bus	0.0553	0.0550	0.54%

N-1 Contingency Voltage Stability Assessment

The N-1 contingency analysis was calculated through the removal of the transmission lines sequentially, the post-contingency power flows, and the bus L- indices were calculated. Table 4. summarizes the results.

The largest L-index of IEEE 14-bus system was 0.1285 when line 20 was out of commission and there were 3 power flow collapses. The worst-case L-index was more severe with the outage of line 41 at 0.1871 using the IEEE 30-bus system and 1 power flow failure. The increased vulnerability of the IEEE 30-bus system to contingency disturbances makes the increased advantage of optimization in larger, more complex networks more likely [3].

Table 4. N-1 Contingency Analysis

Test System	Critical Line	Maximum L-index	PF Failure
IEEE 14 Bus	20	0.1285	3
IEEE 30 Bus	41	0.1871	1

CSO-Based Optimal UPFC Placement Under Contingency

CSO algorithm was run with 20 cats with a population of 50 iterations. The candidate solutions coded four decision variables, including UPFC transmission line location, shunt bus location, series reactance injection Xinj (p.u.) and reactive power injection Qinj (p.u.).

Table 5 reports the best UPFC parameters and resulting minimized worst-case L-indices. In the case of the IEEE 14-bus system, the best UPFC installation was found to be line 7 and Xinj = -0.1000 p.u., Qinj = 0.5000 p.u., and L-index was optimized at 0.1230. For the IEEE 30-bus system, the optimal location was line 40, with Xinj = −0.0988 p.u. and Qinj = −0.3555 p.u., yielding an optimized L-index of 0.1406

ISSN 2278-2540 | DOI: 10.51583/IJLTEMAS | Volume XV, Issue IV, April 2026

Table 5 CSO Results for Optimal UPFC Parameters

Test System index	Optimal Line	Xinj (p.u.)	Qinj (p.u.)	Optimized L-
IEEE 14 Bus	7	-0.1000	0.5000	0.1230
IEEE 30 Bus	40	-0.0988	-0.3555	0.1406

Voltage Stability Improvement Under N-1 Contingency

As shown in Table 6, the CSO-optimized location of the UPFC decreased the worst-case L-index of the IEEE 14-bus system by 0.1285 to 0.1230 representing a 4.28%. The IEEE 30-bus system had a significantly significant decrease of 0.1871 to 0.1406 that represents a 24.85 per cent decrease. The significantly better performance of the larger system validation is that CSO-based UPFC optimization provides more comprehensive security utility in highly complex networks with increased voltage variances and sensitivity to contingencies [6][8][13].

Table 6 Voltage Stability Improvement Analysis (N-1 Contingency)

Test System	Worst Contingency	CSO Optimized (N-1)	Improvement
IEEE 14 Bus	0.1285	0.1230	4.28%
IEEE 30 Bus	0.1871	0.1406	24.85%

CSO Convergence Behavior

Figure 3 (IEEE 14-bus) and Figure 4 (IEEE 30-bus) depict the convergence nature of the CSO algorithm. Both the objective function, worst-case L-index, is reducing with the number of iterations, which proves successful search space exploration. The IEEE 14-bus system has faster convergence rate as it has a smaller and simpler topology, and stabilizes at the level of 0.1230 with 50 iterations. The IEEE 30-bus system shows more oscillations at the beginning stages of the search, as it uses a larger search space, but eventually converges to 0.1406, which supports the convergence to near-optimality. Figure 5 gives the comparative convergence behavior of both systems and shows that the CSO algorithm is robust on networks of varying complexity [10][12].

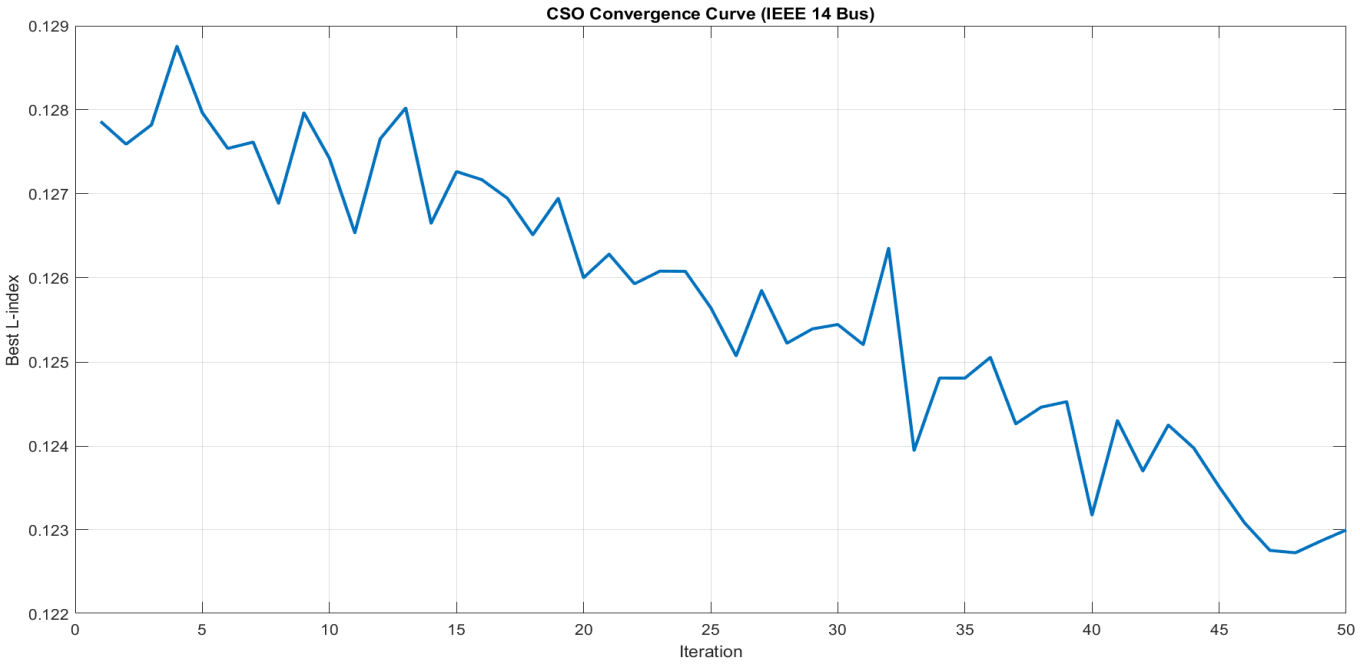

Figure 3 CSO Convergence Curve (IEEE 14 Bus)

ISSN 2278-2540 | DOI: 10.51583/IJLTEMAS | Volume XV, Issue IV, April 2026

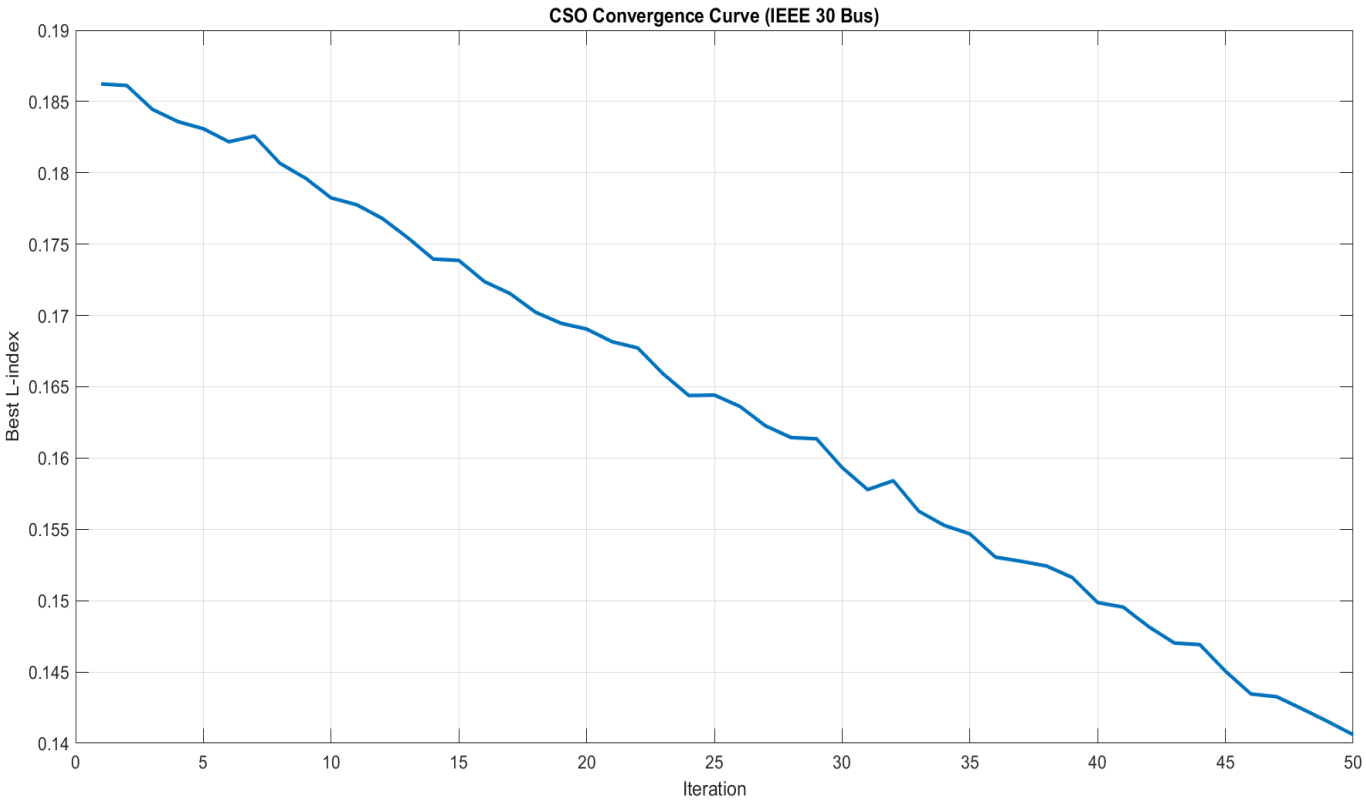

Figure 4. CSO Convergence Curve (IEEE 30 Bus)

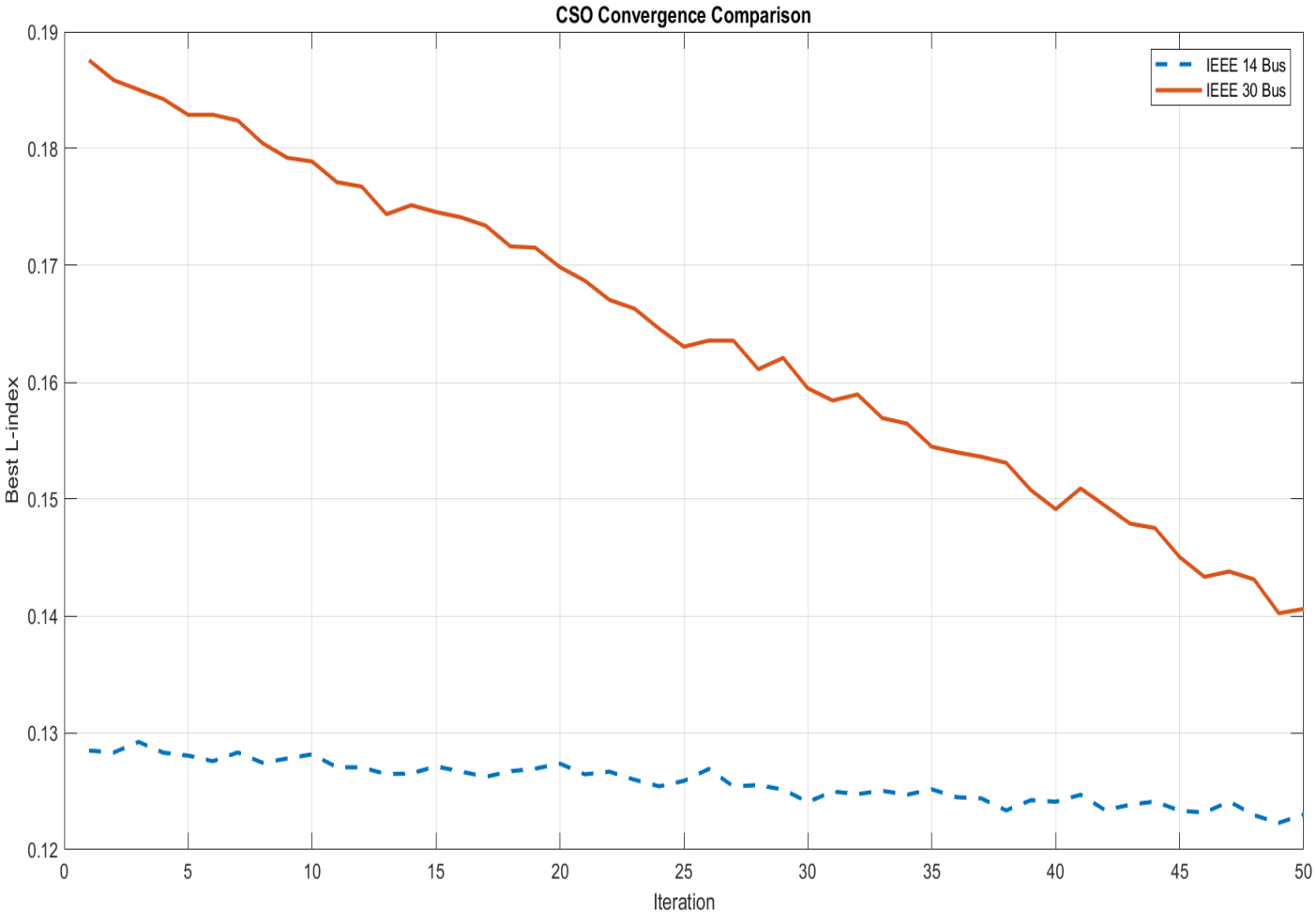

Figure 5 CSO Convergence Comparison

ISSN 2278-2540 | DOI: 10.51583/IJLTEMAS | Volume XV, Issue IV, April 2026

Voltage Profile Improvement

Figure 3 displays bus voltage profile improvement of IEEE 14-bus system, as well as Figure 4. shows bus voltage profile improvement of IEEE 30-bus system. Before optimization, a number of buses were operating at or below the acceptable lower voltage limit of 0.95 p.u. After CSO-optimized UPFC placement, bus voltages were reduced to the nominal 1.0 p.u., and voltage deviations were smaller and the overall profile flatter. This enhancement is greater in the IEEE 30-bus system where formerly weak buses, those with low magnitudes of voltage, had the voltage recovered considerably. These findings attest to the fact that the synchronized series injection and shunt reactive power compensation of the UPFC are effective to control the size of voltages and reassign current flow throughout the network [7]

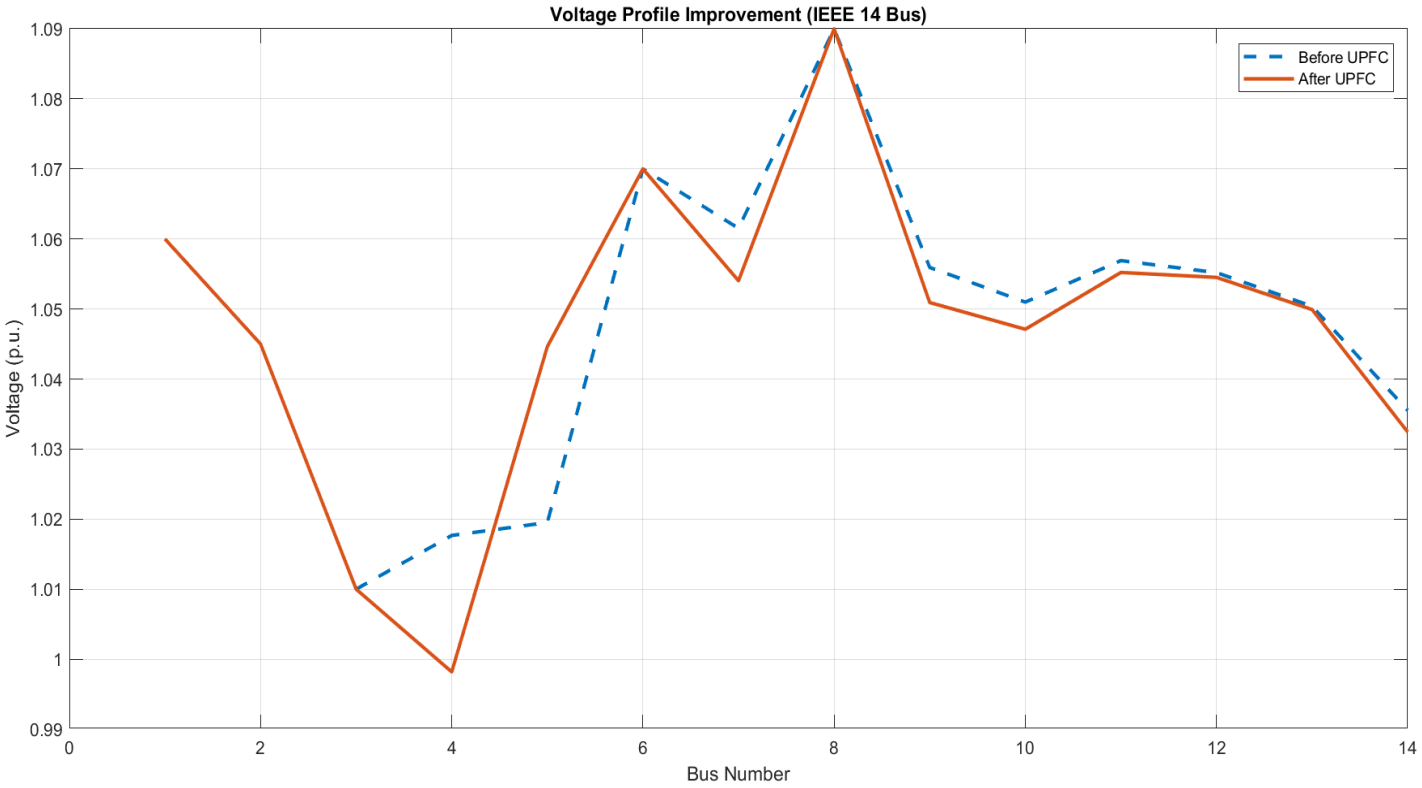

Figure 3. Voltage Profile Improvement (IEEE 14 Bus)

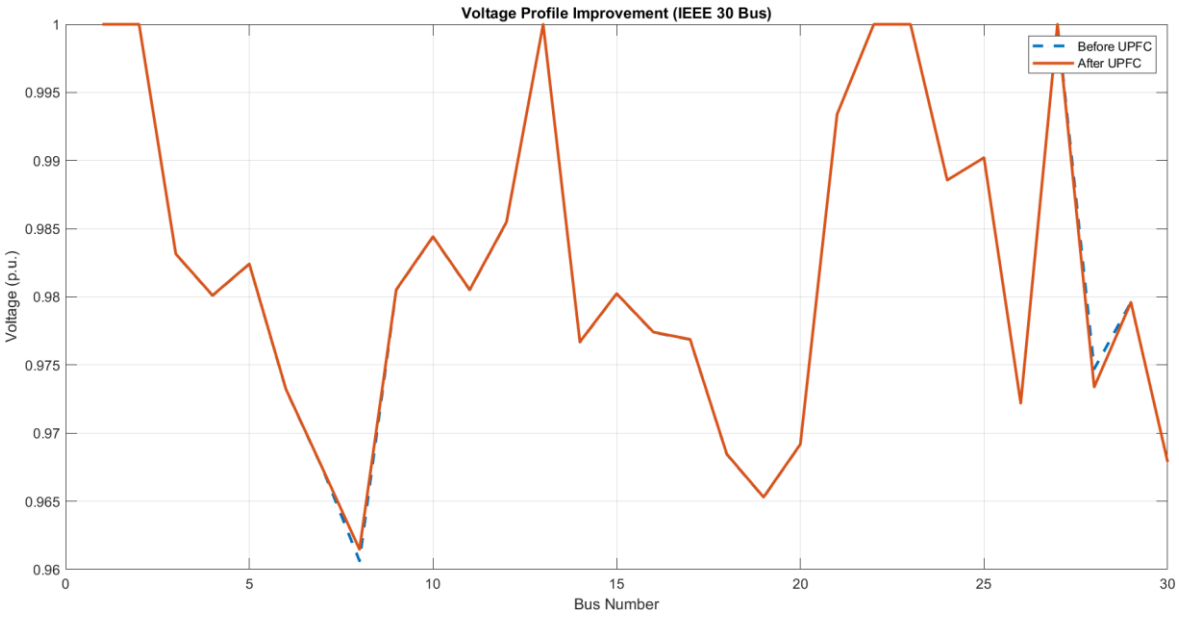

Figure 4. Voltage Profile Improvement (IEEE 30 Bus)

ISSN 2278-2540 | DOI: 10.51583/IJLTEMAS | Volume XV, Issue IV, April 2026

In all the conditions and the two test systems, the outcomes are always the same to indicate that the CSO-based optimal placement of the UPFC helps greatly in improving the power system voltage stability. Both systems had a reduced worst-case L-index, with larger improvements in the larger and more complicated IEEE 30-bus network. Voltage profiles were made positive towards nominal values, reactive power was provided successfully at critical buses and the CSO algorithm showed stable and consistent convergence and did not stop prematurely. These results confirm that the proposed optimization framework makes a valid and computationally efficient approach towards enhancing voltage security under normal and N-1 contingency operating conditions [1][3][16][6][10].

CONCLUSION

This paper introduced a CSO-based optimization model of identifying the optimal location and control settings of the UPFC to enhance voltage stability in the normal and N-1 contingency conditions in the IEEE 14-bus and the IEEE 30-bus benchmark systems. In normal operation, the L-index of IEEE 14-bus and IEEE 30-bus system decreased by 0.26% and 0.54% respectively with UPF integration. Though numerically small, these gains are significant additions to the voltage security margins that are vital at times of high loading and network stress. The results of the N-1 contingency analysis indicated worst-case L-index of 0.1285 and 0.1871 in the IEEE 14-bus and IEEE 30-bus systems respectively which validated the higher susceptibility of larger and more complex networks to single-element disturbances. After placing the optimal UPFC location (CSO optimized) at line 7 and line 40 respectively, the worst-case L-index decreased to 0.1230 and 0.1406 respectively, a 4.28% and 24.85% improvement respectively. The significantly higher gain obtained in the IEEE 30-bus system validates the fact that the offered framework provides bigger security advantages in more complicated and contingency-sensitive networks. The CSO algorithm showed a steady and smooth convergence between the two systems in 50 iterations without any premature stagnation. After optimization, bus voltage profiles moved towards the nominal 1.0 p.u. whereby formerly weak buses had recovered their voltage levels considerably due to the coordinated series reactance injection and shunt reactive power compensation by the UPFC. CSO combined with control in the FACTS-based on UPFC and L-index assessment of voltage stability, which was developed in the MATLAB/MATPOWER framework, is a powerful, gradient-free, and computationally efficient formulation of the optimal FACTS placement problem. This framework has been suggested to be well applicable to larger networks, multi-FACTS setups and dynamic stability improvement under increasingly complex operating conditions of modern power systems.

REFERENCES

1. P. Kundur, Power System Stability and Control. New York, NY, USA: McGraw-Hill, 1994.
2. IEEE/CIGRE Joint Task Force on Stability Terms and Definitions, "Definition and classification of power system stability," IEEE Transactions on Power Systems, vol. 19, no. 2, pp. 1387–1401, May 2004.
3. C. W. Taylor, Power System Voltage Stability. New York, NY, USA: McGraw-Hill, 1994.
4. P. W. Sauer and M. A. Pai, Power System Dynamics and Stability. Upper Saddle River, NJ, USA: Prentice Hall, 1998.
5. N. G. Hingorani, "Flexible AC transmission systems," IEEE Spectrum, vol. 30, no. 4, pp. 40–45, Apr. 1993.
6. L. Gyugyi, "Unified power-flow control concept for flexible AC transmission systems," IEE Proceedings C - Generation, Transmission and Distribution, vol. 139, no. 4, pp. 323–331, Jul. 1992.
7. Y. H. Song and A. T. Johns, Flexible AC Transmission Systems (FACTS). London, U.K.: IEE Press, 1999.
8. X.-P. Zhang, C. Rehtanz, and B. Pal, Flexible AC Transmission Systems: Modelling and Control. Berlin, Germany: Springer, 2006.
9. N. G. Hingorani and L. Gyugyi, Understanding FACTS: Concepts and Technology of Flexible AC Transmission Systems. New York, NY, USA: IEEE Press, 2000.
10. S. C. Chu, P. W. Tsai, and J. S. Pan, "Cat swarm optimization," in Proc. Pacific Rim International Conference on Artificial Intelligence (PRICAI), Guilin, China, Aug. 2006, pp. 854–858.
11. S.-C. Chu and P.-W. Tsai, "Computational intelligence based on the behavior of cats," International Journal of Innovative Computing, Information and Control, vol. 3, no. 1, pp. 163–173, Feb. 2007.

ISSN 2278-2540 | DOI: 10.51583/IJLTEMAS | Volume XV, Issue IV, April 2026

12. A. M. Ahmed, T. A. Rashid, and S. A. M. Saeed, "Cat swarm optimization algorithm: A survey and performance evaluation," Computational Intelligence and Neuroscience, vol. 2020, Art. no. 4854895, pp. 1–20, 2020.
13. G. N. Kumar and M. S. Kalavathi, "Cat swarm optimization for optimal placement of multiple UPFCs in voltage stability enhancement under contingency," International Journal of Electrical Power & Energy Systems, vol. 57, pp. 97–104, 2014.
14. M. A. Abido, "Optimal power flow using particle swarm optimization," International Journal of Electrical Power & Energy Systems, vol. 24, no. 7, pp. 563–571, Oct. 2002.
15. R. D. Zimmerman, C. E. Murillo-Sánchez, and R. J. Thomas, "MATPOWER: Steady-state operations, planning, and analysis tools for power systems research and education," IEEE Transactions on Power Systems, vol. 26, no. 1, pp. 12–19, Feb. 2011.
16. T. Van Cutsem and C. Vournas, Voltage Stability of Electric Power Systems. Boston, MA, USA: Springer, 1998.